

Reading entanglement in terms of spin configurations in quantum magnets

Andrea Fubini^{1,2}, Tommaso Roscilde³, Valerio Tognetti^{2,4,6}, Matteo Tusa², and Paola Verrucchi^{4,5}

¹ MATIS CNR-INFM & Dipartimento di Metodologie Fisiche e Chimiche - Università di Catania, V.le A. Doria 6, I-95125 Catania, Italy

² Dipartimento di Fisica dell'Università di Firenze, Via G. Sansone 1, I-50019 Sesto F.no (FI), Italy

³ Department of Physics and Astronomy, University of Southern California, Los Angeles, CA 90089-0484

⁴ CNR-INFM, UdR Firenze, Via G. Sansone 1, I-50019 Sesto F.no (FI), Italy

⁵ Istituto dei Sistemi Complessi - CNR, Sez. di Firenze via Madonna del Piano, I-50019 Sesto F.no (FI), Italy

⁶ Istituto Nazionale di Fisica Nucleare, Sez. di Firenze, Via G. Sansone 1, I-50019 Sesto F.no (FI), Italy

Received: date / Revised version: date

Abstract. We consider a quantum many-body system made of N interacting $S=1/2$ spins on a lattice, and develop a formalism which allows to extract, out of conventional magnetic observables, the quantum probabilities for any selected spin pair to be in maximally entangled or factorized two-spin states. This result is used in order to capture the meaning of entanglement properties in terms of magnetic behavior. In particular, we consider the concurrence between two spins and show how its expression extracts information on the presence of bipartite entanglement out of the probability distributions relative to specific sets of two-spin quantum states. We apply the above findings to the antiferromagnetic Heisenberg model in a uniform magnetic field, both on a chain and on a two-leg ladder. Using Quantum Monte Carlo simulations, we obtain the above probability distributions and the associated entanglement, discussing their evolution under application of the field.

PACS. 03.67.Mn Entanglement production, characterization, and manipulation – 75.10.Jm Quantized spin models – 05.30.-d Quantum statistical mechanics

1 Introduction

Entanglement properties have recently entered the tool kit for studying magnetic systems, thanks to the insight they provide on aspects which are not directly accessible through the analysis of standard magnetic observables [1,2,3,4,5,6,7]. The analysis of entanglement properties is particularly indicated whenever purely quantum effects come into play, as in the case of quantum phase transitions. However, in order to gain a deeper insight into quantum criticality, as well as into other phenomena such as field-induced factorization [7] and saturation, the connection between magnetic observables and entanglement estimators should be made clearer, a goal we aim at in this paper. On the other hand, most entanglement estimators, as defined for quantum magnetic systems, are expressed in terms of magnetizations and spin correlation functions. It comes therefore natural to wonder where, inside the standard magnetic observables, the information about entanglement is actually stored, and how entanglement estimators can extract it. Quite clearly, by posing this question, one does also address the problem of finding a possible experimental measure of entanglement, which

is of crucial relevance in developing possible solid-state devices for quantum computation.

In this context a privileged role is played by the concurrence C , which measures the entanglement of formation between two q-bits by an expression which is valid not only for pure states but also for mixed ones[8,9]. In the framework of interacting spin systems, exploiting different symmetries of such systems the concurrence has been related to spin-spin correlators and to magnetizations.[10, 11,12,13] However, C has not yet been given a general interpretation from the magnetic point of view, and a genuinely physical understanding of its expression is still elusive.

Scope of this paper is therefore that of giving a simple physical interpretation of bipartite entanglement of formation, building a direct connection between entanglement estimators and occupation probabilities of two-spin states in an interacting spin system. To this purpose we develop a general formalism for analyzing the spin configuration of the system, so as to directly relate it with the expression of the concurrence. The resulting equations are then used to read our data relative to the $S = 1/2$ antiferromagnetic Heisenberg model in a uniform magnetic field, both on a chain and on a two-leg ladder. The model is a cornerstone

in the study of magnetic systems, extensively investigated and quite understood in the zero-field case. When a uniform magnetic field is applied the behavior of the system is enriched, gradually transforming its ground state and thermodynamic behavior. The analysis of entanglement properties in this model, and in particular that referring to the range of pairwise entanglement as field increases, sheds new light not only on the physical mechanism leading to magnetic saturation in low-dimensional quantum systems, but also on the nature of some $T = 0$ transitions observed in bosonic and fermionic systems, such as that of hard-core bosons with Coulomb interaction, and that described by the bond-charge extended Hubbard model, respectively. In the former case, the connection between magnetic and bosonic model is obtained by an exact mapping that allows a straightforward generalization of our results to the discussion of the phase diagram of the strongly interacting boson-Hubbard model [14]. In the more complex case of the the bond-charge extended Hubbard model, a direct connection between the Heisenberg antiferromagnet in a field is not formally available, but a recent work by Anfossi *et al.*[15] has shown that some of the $T = 0$ transitions observed in the system are characterized by long-ranged pairwise entanglement of the same type we observe in our magnetic model at saturation.

Our data result from stochastic series expansion (SSE) quantum Monte Carlo simulations based on the directed-loop algorithm[16]. The calculations were carried on a chain with size $L = 64$ and on a $L \times 2$ ladder with $L = 40$. In order to capture the ground-state behavior we have considered inverse temperatures $\beta = 2L$.

In Sec.2 we define the magnetic observables we refer to, and develop the formalism which allows us to write them in terms of probabilities for two spins to be in specific states, both at zero and at finite temperature. In Sec. 3 we show how concurrence extracts, out of the above probabilities, the specific information on bipartite entanglement of formation. In Secs. 4 and 5 we present our SSE data for the antiferromagnetic Heisenberg model on a chain and on a square ladder respectively, and read them in light of the discussion of Secs. 2 and 3. Conclusions are drawn in Sec. 6.

2 From magnetic observables to spin configurations

We study a magnetic system made of N spins $S = 1/2$ sitting on a lattice. Each spin is described by a quantum operator \mathbf{S}_l , with $[S_l^\alpha, S_m^\beta] = i\delta_{lm}\varepsilon_{\alpha\beta\gamma}S_l^\gamma$, l and m being the site-indexes.

The magnetic observables we consider are the local magnetization along the quantization axis:

$$M_l^z \equiv \langle S_l^z \rangle, \quad (1)$$

and the correlation functions between two spins sitting on sites l and m :

$$g_{lm}^{\alpha\alpha} \equiv \langle S_l^\alpha S_m^\alpha \rangle. \quad (2)$$

The averages $\langle \cdot \rangle$ represent expectation values over the ground state for $T = 0$, and thermodynamic averages for $T > 0$.

We now show that the above single-spin and two-spin quantities provide a direct information on the specific quantum state of any two spins of the system. Let us consider the $T = 0$ case first: For a lighter notation we drop site-indexes, allowing their appearance whenever needed. After selecting two spins, sitting on sites l and m , any pure state of the system may be written as

$$|\Psi\rangle = \sum_{\nu \in \mathcal{S}} |\nu\rangle \sum_{\Gamma \in \mathcal{R}} c_{\nu\Gamma} |\Gamma\rangle, \quad (3)$$

where \mathcal{S} is an orthonormal basis for the 4-dimensional Hilbert space of the selected spin pair, while \mathcal{R} is an orthonormal basis for the 2^{N-2} -dimensional Hilbert space of the rest of the system. Moreover, in order to simplify the notation, we understand products of kets relative to (operators acting on) different spins as tensor products, meanwhile dropping the corresponding symbol \otimes . The quantum probability for the spin pair to be in the state $|\nu\rangle$, being the system in the pure state $|\Psi\rangle$, is $p_\nu \equiv \sum_{\Gamma} |c_{\nu\Gamma}|^2$, and the normalization condition $\langle \Psi | \Psi \rangle = 1$ implies $\sum_{\nu} p_\nu = 1$.

We consider three particular bases for the spin pair:

$$\mathcal{S}_1 \equiv \{|u_I\rangle, |u_{\text{II}}\rangle, |u_{\text{III}}\rangle, |u_{\text{IV}}\rangle\}, \quad (4)$$

$$\mathcal{S}_2 \equiv \{|e_1\rangle, |e_2\rangle, |e_3\rangle, |e_4\rangle\}, \quad (5)$$

$$\mathcal{S}_3 \equiv \{|u_I\rangle, |u_{\text{II}}\rangle, |e_3\rangle, |e_4\rangle\}, \quad (6)$$

with

$$\begin{aligned} |u_I\rangle &\equiv |\uparrow\rangle_l |\uparrow\rangle_m, & |u_{\text{II}}\rangle &\equiv |\downarrow\rangle_l |\downarrow\rangle_m, \\ |u_{\text{III}}\rangle &\equiv |\uparrow\rangle_l |\downarrow\rangle_m, & |u_{\text{IV}}\rangle &\equiv |\downarrow\rangle_l |\uparrow\rangle_m, \\ |e_1\rangle &= \frac{1}{\sqrt{2}} (|u_I\rangle + |u_{\text{II}}\rangle), & |e_2\rangle &= \frac{1}{\sqrt{2}} (|u_I\rangle - |u_{\text{II}}\rangle), \\ |e_3\rangle &= \frac{1}{\sqrt{2}} (|u_{\text{III}}\rangle + |u_{\text{IV}}\rangle), & |e_4\rangle &= \frac{1}{\sqrt{2}} (|u_{\text{III}}\rangle - |u_{\text{IV}}\rangle), \end{aligned} \quad (7)$$

where $|\uparrow\rangle_{l,m}$ ($|\downarrow\rangle_{l,m}$) are eigenstates of $S_{l,m}^z$ with eigenvalue $+\frac{1}{2}$ ($-\frac{1}{2}$). For the coefficients entering Eq. (3), and for each state Γ , the following relations hold

$$c_{1\Gamma} = \frac{1}{\sqrt{2}} (c_{I\Gamma} + c_{\text{II}\Gamma}), \quad c_{2\Gamma} = \frac{1}{\sqrt{2}} (c_{I\Gamma} - c_{\text{II}\Gamma}), \quad (8)$$

$$c_{3\Gamma} = \frac{1}{\sqrt{2}} (c_{\text{III}\Gamma} + c_{\text{IV}\Gamma}), \quad c_{4\Gamma} = \frac{1}{\sqrt{2}} (c_{\text{III}\Gamma} - c_{\text{IV}\Gamma}), \quad (9)$$

meaning also

$$|c_{1\Gamma}|^2 + |c_{2\Gamma}|^2 = |c_{I\Gamma}|^2 + |c_{\text{II}\Gamma}|^2, \quad (10)$$

$$|c_{1\Gamma}|^2 - |c_{2\Gamma}|^2 = |c_{I\Gamma} c_{\text{II}\Gamma}| \cos(\varphi_I^\Gamma - \varphi_{\text{II}}^\Gamma), \quad (11)$$

$$|c_{3\Gamma}|^2 + |c_{4\Gamma}|^2 = |c_{\text{III}\Gamma}|^2 + |c_{\text{IV}\Gamma}|^2, \quad (12)$$

$$|c_{3\Gamma}|^2 - |c_{4\Gamma}|^2 = |c_{\text{III}\Gamma} c_{\text{IV}\Gamma}| \cos(\varphi_{\text{III}}^\Gamma - \varphi_{\text{IV}}^\Gamma), \quad (13)$$

where $c_{\nu\Gamma} \equiv |c_{\nu\Gamma}| e^{i\varphi_\nu^\Gamma}$.

According to the usual nomenclature \mathcal{S}_1 and \mathcal{S}_2 are the *standard* and *Bell* bases, respectively, while \mathcal{S}_3 is here called the *mixed* basis. Such bases are characterized by the fact that states corresponding to parallel and antiparallel spins do not mix with each other. It therefore makes sense

to refer to $|u_I\rangle, |u_{\text{II}}\rangle, |e_1\rangle$, and $|e_2\rangle$ as *parallel states*, and to $|u_{\text{III}}\rangle, |u_{\text{IV}}\rangle, |e_3\rangle$, and $|e_4\rangle$ as *antiparallel states*. The probabilities specifically related with the elements of \mathcal{S}_1 will be hereafter indicated by $p_I, p_{\text{II}}, p_{\text{III}}$, and p_{IV} while p_1, p_2, p_3 , and p_4 will be used for those relative to the elements of \mathcal{S}_2 . From the normalization conditions

$$p_I + p_{\text{II}} + p_{\text{III}} + p_{\text{IV}} = 1 \quad (14)$$

$$p_1 + p_2 + p_3 + p_4 = 1 \quad (15)$$

$$p_I + p_{\text{II}} + p_3 + p_4 = 1, \quad (16)$$

or equivalently from Eqs. (10) and (12), follows $p_I + p_{\text{II}} = p_1 + p_2$, and $p_{\text{III}} + p_{\text{IV}} = p_3 + p_4$, representing the probability for the two spins to be parallel and antiparallel, respectively. We do also notice that the elements of \mathcal{S}_1 are factorized states, while those of \mathcal{S}_2 are maximally entangled ones.

The above description is easily translated in terms of the two-site reduced density matrix

$$\rho = \sum_{\Gamma} \langle \Gamma | \Psi \rangle \langle \Psi | \Gamma \rangle = \sum_{\nu\lambda} |\nu\rangle \langle \lambda| \sum_{\Gamma} c_{\nu\Gamma} c_{\mu\Gamma}^*, \quad (17)$$

whose diagonal elements are the probabilities for the elements of the basis chosen for writing ρ . The normalization conditions Eqs. (14-16) translate into $\text{Tr}(\rho) = 1$.

Thanks to the above parametrization, the magnetic observables (1) and (2) are directly connected to the probabilities of the two spins being in one of the states (7). In fact it is

$$\begin{aligned}
2(g^{xx} + g^{yy}) &= \langle \Psi | S_l^+ S_m^- + S_l^- S_m^+ | \Psi \rangle = \\
&= \langle \Psi | S_l^+ S_m^- + S_l^- S_m^+ | \left(|e_3\rangle \sum_{\Gamma} c_{3\Gamma} |\Gamma\rangle + |e_4\rangle \sum_{\Gamma} c_{4\Gamma} |\Gamma\rangle \right) \rangle = \\
&= \langle \Psi | \left(|e_3\rangle \sum_{\Gamma} c_{3\Gamma} |\Gamma\rangle - |e_4\rangle \sum_{\Gamma} c_{4\Gamma} |\Gamma\rangle \right) \rangle \\
&= (p_3 - p_4) , \tag{18}
\end{aligned}$$

and similarly

$$2(g^{xx} - g^{yy}) = (p_1 - p_2) , \quad (19)$$

$$g^{zz} = \frac{1}{2}(p_1 + p_{\text{II}}) - \frac{1}{4} = \frac{1}{2}(p_1 + p_2) - \frac{1}{4} , \quad (20)$$

$$M_z \equiv \frac{1}{2}(M_l^z + M_m^z) = (p_1 - p_{\text{II}}) , \quad (21)$$

where all S_i are suitable to calculate g^{zz} , while $(g^{xx} \pm g^{yy})$ and M_z specifically require \mathcal{S}_2 and \mathcal{S}_3 , respectively. After Eqs. (18)-(21), one finds

$$p_1 = \frac{1}{4} + g^{zz} + M_z , \quad (22)$$

$$p_{\text{II}} = \frac{1}{4} + g^{zz} - M_z , \quad (23)$$

$$p_1 = \frac{1}{4} + g^{xx} - g^{yy} + g^{zz} , \quad (24)$$

$$p_2 = \frac{1}{4} - g^{xx} + g^{yy} + g^{zz} , \quad (25)$$

$$p_3 = \frac{1}{4} + g^{xx} + g^{yy} - g^{zz} , \quad (26)$$

$$p_4 = \frac{1}{4} - g^{xx} - g^{yy} - g^{zz} . \quad (27)$$

It is to be noticed that the probabilities relative to the Bell states do not depend on the magnetization.

In the the finite temperature case, the generalization is straightforwardly obtained by writing each of the Hamiltonian eigenstates, numbered by the index n , in the form (3), so that

$$\rho(T) = \sum_{\nu\mu} |\nu\rangle\langle\mu| \sum_n e^{-E_n/T} \sum_{\Gamma} c_{\nu\Gamma,n} c_{\mu\Gamma,n}^* . \quad (28)$$

In terms of probabilities the above expression simply means that the purely quantum p_{μ} shall be replaced by the quantum statistical probabilities

$$p_{\mu}(T) \equiv \sum_n e^{-E_n/T} \sum_{\Gamma} |c_{\nu\Gamma,n}|^2 . \quad (29)$$

Therefore, apart from the further complication of the formalism, the discussion developed for pure states stays substantially unchanged when $T > 0$.

Equations (22)-(27) show that magnetic observables allow a certain insight into the spin configuration of the system, as they give, when properly combined, the probabilities for any selected spin pair to be in some specific quantum state. However, the mere knowledge of such probabilities is not sufficient to appreciate the quantum character of the global state, and more specifically to quantify its entanglement properties.

3 From spin configurations to entanglement properties

We here analyze the entanglement of formation[17,8,9] between two spins, quantified by the concurrence C . In the simplest case of two isolated spins in the pure state $|\phi\rangle$ the concurrence may be written as $C = |\sum_i \alpha_i^2|$, where α_i are the coefficients entering the decomposition of $|\phi\rangle$ upon the magic basis $\{|e_1\rangle, |i|e_2\rangle, |i|e_3\rangle, |e_4\rangle\}$. However, if one refers

to the notation of the previous section, it is easily shown that

$$C(|\phi\rangle) = |(c_1^2 - c_2^2) - (c_3^2 - c_4^2)| = 2|c_{\text{I}}c_{\text{II}} - c_{\text{III}}c_{\text{IV}}| , \quad (30)$$

where Eqs. (8)-(9) have been used, with index Γ obviously suppressed. The above expression shows that C extracts the information about the entanglement between the two spins by combining probabilities and phases relative to specific two-spin state.

In fact, one should notice that a finite probability for two spins to be in a maximally entangled state does not guarantee *per se* the existence of entanglement between them, since this probability may be finite even if the two spins are in a separable state.[18] In a system with decaying correlations, at infinite separation all probabilities associated to Bell states attain the value of 1/4, but this of course tells nothing about the entanglement between them, which is clearly vanishing. It is therefore expected that *differences* between such probabilities, rather than the probabilities themselves give insight in the presence or absence of entanglement.

When the many-body case is tackled, the mixed-state concurrence of the selected spin pair has an involved definition in terms of the reduced two-spin density matrix.[9] However, possible symmetries of the Hamiltonian \mathcal{H} greatly simplify the problem to the extent that C results a simple function of the probabilities (22)-(27) only. We here assume that \mathcal{H} is real, has parity symmetry (meaning that either \mathcal{H} leaves the z component of the total magnetic moment unchanged, or changes it in steps of 2), and is further characterized by translational and site-inversion invariance. The two latter properties implies M_l^z as defined in Eq. (1) to coincide with the uniform magnetization $M_z \equiv \sum_l \langle S_l^z \rangle / N$, and the probabilities $p_{\text{III}} = p_{\text{IV}}$, respectively.

Under these assumptions, the concurrence for a given spin pair is[13]

$$C_{(r)} \equiv 2 \max\{0, C'_{(r)}, C''_{(r)}\} , \quad (31)$$

$$C'_{(r)} \equiv |g_{(r)}^{xx} + g_{(r)}^{yy}| - \sqrt{\left(\frac{1}{4} + g_{(r)}^{zz}\right)^2 - M_z^2} , \quad (32)$$

$$C''_{(r)} \equiv |g_{(r)}^{xx} - g_{(r)}^{yy}| - \frac{1}{4} + g_{(r)}^{zz} , \quad (33)$$

where r is the distance in lattice units between the two selected spins. Despite being simple combinations of magnetic observables, the physical content of the above expressions is not straightforward. However, by using the expression found in Section 2, one can write Eqs. (32) and (33) in terms of the probabilities for the two spins to be in maximally entangled or factorized states, thus finding, in some sense, an expression which is analogous to Eq. (30) for the case of mixed states. In fact, from Eqs. (18)-(19), it follows

$$2C' = |p_3 - p_4| - 2\sqrt{p_{\text{I}}p_{\text{II}}} , \quad (34)$$

$$\begin{aligned} 2C'' &= |p_1 - p_2| - (1 - p_1 - p_2) = \\ &= |p_1 - p_2| - 2\sqrt{p_{\text{III}}p_{\text{IV}}} , \end{aligned} \quad (35)$$

where we have used $p_{\text{III}}=p_{\text{IV}}$ and hence $p_3 + p_4 = 2p_{\text{III}} = 2\sqrt{p_{\text{III}}p_{\text{IV}}}$. The expression for C'' may be written in the particularly simple form

$$2C'' = 2\max\{p_1, p_2\} - 1, \quad (36)$$

telling us that, in order for C'' to be positive, it must be either $p_1 > 1/2$ or $p_2 > 1/2$. This means that one of the two parallel Bell states needs to saturate at least half of the probability, which implies that it is by far the state where the spin pair is most likely to be found.

Despite the apparently similar structure of Eqs. (34) and (35), understanding C' is more involved, due to the fact that $\sqrt{p_1 p_{\text{II}}}$ cannot be further simplified unless $p_1 = p_{\text{II}}$. The marked difference between C' and C'' reflects the different mechanism through which parallel and antiparallel entanglement is generated when time reversal symmetry is broken, meaning $p_1 \neq p_{\text{II}}$ and hence $M_z \neq 0$. In fact, in the zero magnetization case, it is $p_{\text{II}} = p_1 = (p_1 + p_2)/2$ and hence

$$2C' = 2\max\{p_3, p_4\} - 1, \quad (37)$$

which is fully analogous to Eq. (36), so that the above analysis can be repeated by simply replacing p_1 and p_2 with p_3 and p_4 .

For $M_z \neq 0$, the structure of Eq. (37) is somehow kept by introducing the quantity

$$\Delta^2 \equiv (\sqrt{p_1} - \sqrt{p_{\text{II}}})^2, \quad (38)$$

so that

$$2C' = 2\max\{p_3, p_4\} - (1 - \Delta^2), \quad (39)$$

meaning that the presence of a magnetic field favors bipartite entanglement associated to antiparallel Bell states, $|e_3\rangle$ and $|e_4\rangle$. In fact, when time reversal symmetry is broken the concurrence can be finite even if $p_3, p_4 < 1/2$.

From Eqs. (36) and (39) one can conclude that, depending on C being finite due to C' or C'' , the entanglement of formation originates from finite probabilities for the two selected spins to be parallel or antiparallel, respectively. In this sense we will speak about *parallel* and *antiparallel* entanglement.

Moreover, from Eqs. (34)-(35) we notice that, in order for parallel (antiparallel) entanglement to be present in the system, the probabilities for the two parallel (antiparallel) Bell states must be not only finite but also different from each other. Thus, the Bell states $|e_1\rangle$ and $|e_2\rangle$ ($|e_3\rangle$ and $|e_4\rangle$) result mutually exclusive in the formation of entanglement between two spins in the system, the latter being present only if one of the Bell state is more probable than the others. The case $p_1 = p_2 = 1/2$ ($p_3 = p_4 = 1/2$) corresponds in turn to an incoherent mixture of $|e_1\rangle$ and $|e_2\rangle$ ($|e_3\rangle$ and $|e_4\rangle$).

In fact, the occurrence of the differences $|p_1 - p_2|$ and $|p_3 - p_4|$ is intriguing. Let us comment on $|p_1 - p_2|$, as the same kind of analysis holds for $|p_3 - p_4|$. In the general case the difference $p_1 - p_2$ can vanish because of genuine many-body effects which are not directly readable in terms of 2-spin entangled or separable states. It is easier to interpret Eq. (35) [Eq. (34)], if one restricts the possibilities to the

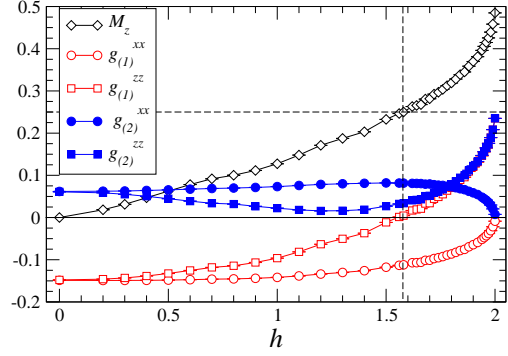


Fig. 1. Magnetization and correlators versus the magnetic field h for the chain Eq. (40). The dashed lines mark the value of the field where $p_{\text{II}} = 0$ (see text).

case in which the two spins are not entangled with the rest of the system. By using Eq. (11), one can select two particular situations all leading to $p_1 = p_2$:

- (i) $c_{1\Gamma}$ or $c_{\text{II}\Gamma}$ vanishes $\forall \Gamma$, meaning that $|\Psi\rangle$ does not contain states where the two selected spins are parallel and entangled;
- (ii) for each Γ such that both $|c_{1\Gamma}|$ and $|c_{\text{II}\Gamma}|$ are non-zero, it is $\varphi_1^\Gamma - \varphi_{\text{II}}^\Gamma = \pi/2$. Thus, whatever the antiparallel components are, the parallel terms of $|\Psi\rangle$ appear in the form $(\alpha|e_1\rangle + \alpha^*|e_2\rangle)$.

The above analysis suggests the first term in C'' (C') to distill, out of all possible parallel (antiparallel) spin configurations, those which are specifically related with entangled parallel (antiparallel) states. These characteristics reinforce the meaning of what we have called parallel and antiparallel entanglement.

4 Chain

We consider the isotropic Heisenberg antiferromagnetic chain in a uniform magnetic field, described by

$$\frac{\mathcal{H}}{J} = \sum_i \mathbf{S}_i \cdot \mathbf{S}_{i+1} - h S_i^z, \quad (40)$$

where the exchange integral J is positive, and the reduced magnetic field $h \equiv g\mu_B H/J$ is assumed uniform.

This model is characterized by the rotational symmetry on the xy plane, as well as by the existence of a saturation field $h_s = 2$, such that for $h \geq h_s$ the ground state is the factorized ferromagnetic one, with all spins aligned along the field direction. Moreover, Eq. (40) has all the necessary symmetries for Eqs. (31)-(33) to hold.

Due to the rotational symmetry on the xy plane, it is $g^{xx} = g^{yy}$, meaning $p_1 = p_2 = \frac{1}{4} + g^{zz} \leq 1/2$, according to Eqs. (24) and (25), and hence null parallel entanglement ($C'' \leq 0$) between any two spins along the chain, no matter the field, the temperature, and the distance between them.

In Fig. 1 we show the $T = 0$ correlation functions for nearest neighboring (n.n.) and next-nearest neighboring (n.n.n.) spins, together with the uniform magnetization,

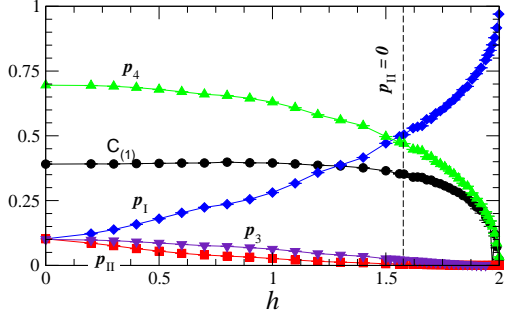


Fig. 2. Concurrence and related probabilities of the mixed basis states \mathcal{S}_3 [Eq. (6)] for n.n. sites of the chain Eq. (40)

as the field is varied. Beyond the overall regular behavior, we notice that there exists a value of the magnetic field where one simultaneously observes $g_{(1)}^{zz} = 0$ and $M_z = 1/4$ (indicated by the dashed lines). According to Eqs. (20) and (21) this implies null probability $p_{||}$ for adjacent spins to be parallel in the direction opposite to the field. This means that the ground-state configuration is a superposition of spin configurations entirely made of stable clusters of spins parallel to the field separated by Néel-like strings.

In Fig. 2 we show the probabilities for n.n. spins to be in the states of the mixed basis, together with the n.n. concurrence: The value of the n.n. concurrence for $h = 0$ is in agreement with the exact result in the thermodynamic limit.[12] In presence of an external magnetic field, $C_{(1)}$ is found positive $\forall h$, meaning that, no matter the value of the field, the probabilities p_3 and p_4 for adjacent spins are always different from each other. The probabilities for the triplet states $|e_3\rangle, |u_{||}\rangle$, and $|u_{\perp}\rangle$ are equal for $h = 0$ and depart from each other when the field is switched on. The singlet $|e_4\rangle$ evidently dominates the ground state up to a field which roughly corresponds to the value where $p_{||}$ vanishes.

As for the concurrence, despite the ground-state structure evidently changes as the field increases, $C_{(1)}$ stays substantially constant up to a large value of the field, mainly due to the fact that not only p_4 but also p_3 decreases with the field. This behavior mimics the one occurring in a spin dimer, whose ground state is the singlet state $|e_4\rangle$ up to $h = 1$ where, after a level crossing, $|u_{\perp}\rangle$ becomes energetically favored. However, in a spin chain, many-body effects smear the sharp behavior of the dimer due to the level crossing. We do also notice that $C_{(1)}$ starts to decrease as soon as the total probability for parallel spins ($p_1 + p_{||}$) gets larger than that for antiparallel spins ($p_3 + p_4$). The further reduction of $C_{(1)}$ is mainly driven by p_1 starting to rapidly increase.

In the same field region where a substantial change in the n.n. configuration occurs, the n.n.n. concurrence $C_{(2)}$ switches on. This is seen in Fig. 3, where the probabilities for n.n.n. spins are shown together with the corresponding concurrence. In fact, when considering the n.n.n. quantities, we notice that both $g_{(2)}^{xx}$ and $g_{(2)}^{zz}$ have a non-monotonic behavior, displaying a maximum and a mini-

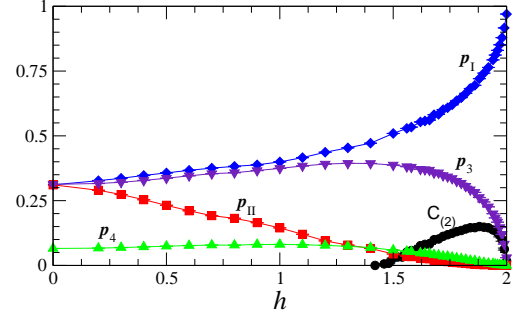


Fig. 3. Concurrence and related probabilities of the mixed basis states \mathcal{S}_3 [Eq. (6)] for n.n.n. sites of the chain Eq. (40).

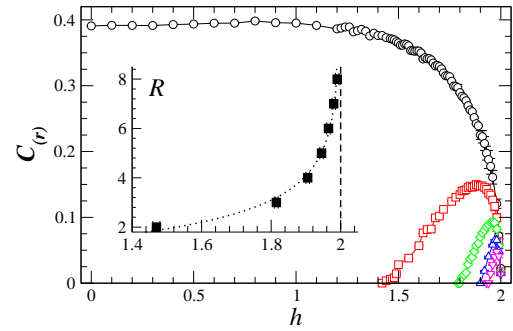


Fig. 4. From the upper to the lower curves: concurrences from the nearest- up to the 5th-neighbors of the chain Eq. (40). The inset shows the divergence of the range of the concurrence as $h \rightarrow h_s$, the line shows the $(h - h_s)^{-1/2}$ behavior.

imum, respectively, in the field region where $C_{(2)}$ gets positive (as from the comparison between Fig. 1 and 3).

Regarding the probabilities, one finds that, although the most likely state is always $|u_{\perp}\rangle$, p_3 is surprisingly large, and almost equal to p_1 , as far as $h < 1$. Moreover, both p_3 and p_4 have a non monotonic behavior and increase with h up to the field where we simultaneously observe $g_{(2)}^{xx}$ and $g_{(2)}^{yy}$ attaining their extreme values, p_1 exceeding $1/2$, p_4 getting larger than $p_{||}$, and $C_{(2)}$ switching on.

As observed in the n.n. case, when $p_{||}$ for n.n.n. spins vanishes $C_{(3)}$ switches on. Let us further comment upon $C_{(1)}$, $C_{(2)}$, and $C_{(3)}$. Given the fact that only antiparallel entanglement may exist in this chain, it is not surprising that $C_{(1)} > 0$ and $C_{(2)} = 0$ at low fields, as n.n. spins belong to different sublattices, while n.n.n. spins belong to the same sublattice. However, the fact that $C_{(2)}$ becomes finite indicates a ground-state evolution from the Néel-like to the ferromagnetic state such that the system enters a region where quantum fluctuations increase the total probability for spins belonging to the same sublattice to be antiparallel and entangled. The opposite effect is understood when $C_{(3)}$ is considered: in order to keep $C_{(3)} = 0$ almost up to the saturation field, quantum fluctuations must reduce the total probability for spins belonging to different sublattices to be antiparallel and entangled.

The above comments upon $C_{(2)}$ and $C_{(3)}$ may be generalized to $C_{(n)}$ with even and odd n , respectively. In Fig. 4 we in fact show C_n up to $n = 5$. The concurrence for in-

creasing distance between the two spins gets finite for a big enough field resembling the phenomenology of finite spin clusters.[1] Moreover, combining the exact results of Refs.[19] and [20], we find that the range of the concurrence for the model (40), namely the distance R such that $C_{(r)}$ vanishes for $r > R$, is

$$R = \left| \frac{\rho}{\sqrt{\pi}(2 + 4M_z)(\frac{1}{2} - M_z)^{1/2}} \right|^\theta, \quad (41)$$

with the constant $\rho = 0.924\dots$. When $h \rightarrow h_s$, it is $M_z \simeq \frac{1}{2} - \frac{\sqrt{2}}{\pi}\sqrt{h_s - h}$ and $\theta \simeq 2 - \frac{2\sqrt{2}}{\pi}\sqrt{h_s - h}$, and the range of the concurrence is seen to diverge according to $R \simeq \frac{\rho\sqrt{2}}{32}(h_s - h)^{-1/2}$. In other terms, approaching the saturation field, all $C_{(n)}$ become finite of order $O(1/N)$, consistently with the occurrence of a $|W_N\rangle$ state[21]. For such state the entanglement is maximally bipartite in the sense of the Coffman-Kundu-Wootters inequality.[21,22,23] This scenario is consistent with our numerical data. As shown in Fig.4 up to $n = 5$, for any $C_{(n)}$ it exists a field $h_n > h_{n-1}$ such that $C_{(n)}$ is positive for $h \in [h_n, 2)$, with $h_n \rightarrow 2$ for $n \rightarrow \infty$. The divergence of the range of the concurrence for $h \rightarrow h_s$ is shown in the inset of Fig. 4. Although the correct power-law behavior shows up, the precision of the numerical data is not sufficient to get the correct multiplicative constant. In fact, the above expression (41) is derived from asymptotic exact results, valid only for $r \gg 1$, when $C_{(r)}$ becomes too small to resolve it numerically.

The formalism introduced in the previous sections works also in the finite temperature case, where it describes the effects of thermal fluctuations on quantum coherence. In Fig. 5, the temperature dependence of probabilities and concurrences, for $h = 1.8$, shows how thermal fluctuations progressively drive the system towards an incoherent mixture of states. Increasing T the concurrences (right panel) are progressively suppressed and above $k_B T \sim 0.8J$ also the n.n. concurrence vanishes. At higher temperatures none of the spin pairs in the system is entangled and quantum coherence is lost. The temperature behavior of the probabilities (left panel) is non monotonic, signaling the relative weight of the different states in the energy spectrum of the system. Eventually, at high T all the probabilities tends to the asymptotic value $p_\nu = 1/4$.

5 Two-Leg Ladder

The above picture further enriches when considering the two-leg isotropic ladder, described by

$$\frac{\mathcal{H}}{J} = \sum_i \sum_{\alpha=0,1} (\mathbf{S}_{i,\alpha} \cdot \mathbf{S}_{i+1,\alpha} - h S_{i,\alpha}^z) + \gamma \mathbf{S}_{i,0} \cdot \mathbf{S}_{i,1}, \quad (42)$$

where the index i runs on both the right ($\alpha = 0$) and left ($\alpha = 1$) leg. The first term is the Heisenberg Hamiltonian (40) for the right and left legs, while the last term describes the exchange interaction between spins of the same rung, whose relative weight is γ .

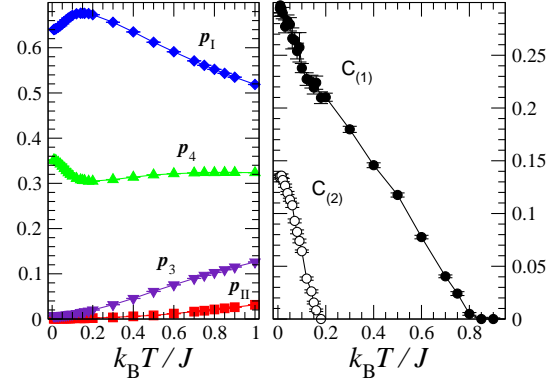


Fig. 5. Left panel: n.n. probabilities versus temperature at $h = 1.8$. Right panel: n.n. and n.n.n. concurrences versus temperature at $h = 1.8$.

The model (42) is known to describe cuprate compounds like SrCu_2O_3 and it has been extensively studied for zero[24,25] and finite field[26]. The system shows a gap Δ in the excitation spectrum that can be interpreted essentially as due to the energy cost for producing a triplet excitation on a rung [24]. The system reaches full polarization[26], with all spins aligned along the field direction, for $h > \gamma + 2$.

In the following we will specifically consider the isotropic case $\gamma = 1$, which is characterized by a gap $\Delta \approx 0.5J$,[24] and by a saturation field $h_s = 3$. As in the chain case, due to the rotational invariance on the xy plane, parallel entanglement cannot develop in the isotropic ladder. On the other hand, antiparallel bipartite entanglement can here develop between spins belonging to the same leg, or to the same rung, or to a different rung and leg. Two-spin quantities will be hereafter pinpointed by the two-component vector (r_i, r_α) joining the two selected spins, the first component referring to the direction of the legs, and the second one to that of the rungs. The indexes (01), (10), (11), (20) will therefore indicate n.n. spins on the same rung, n.n. along one leg, n.n.n. on adjacent rungs, and n.n.n. along the same leg, respectively.

Our SSE data in Fig. 6 for the uniform magnetization and the n.n. correlation functions $g_{(01)}^{\alpha\alpha}$, $g_{(10)}^{\alpha\alpha}$ confirm the description given in the previous paragraph: Before the Zeeman interaction fills the energy gap at the critical value $h_c \simeq 0.5$, the ground-state configuration is frozen and characterized by the singlet $|e_4\rangle$ being by far the most likely state for each rung.

The use of the formalism developed in Sec. 2 gives a direct information on the physics of the system: In Fig. 7 we see that the singlet probabilities p_4 relative to n.n. spins on a rung and along one leg, as functions of the field, share a similar behavior everywhere but at the critical field h_c , where p_4 for n.n. spins sitting on the same rung shows up a kink that is not present in the singlet probability along the leg. This qualitatively different behavior clearly reflects the nature of the energy gap that closes at h_c . The sharp decrease of p_4 in favor of p_1 on the rung just above h_c testifies that, even in the case, here considered, of equal exchange interaction along the legs and on the

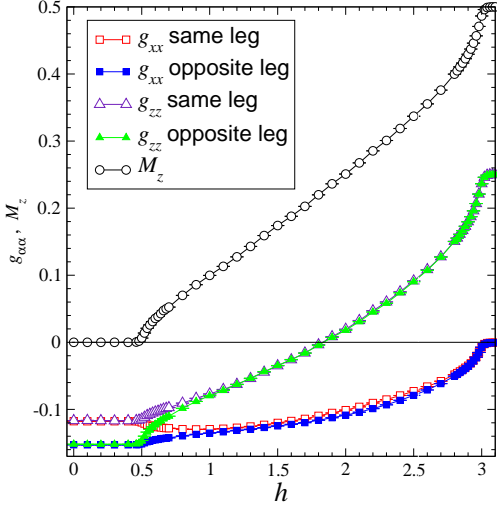


Fig. 6. Magnetization and correlators versus the magnetic field h for the ladder Eq. (42).

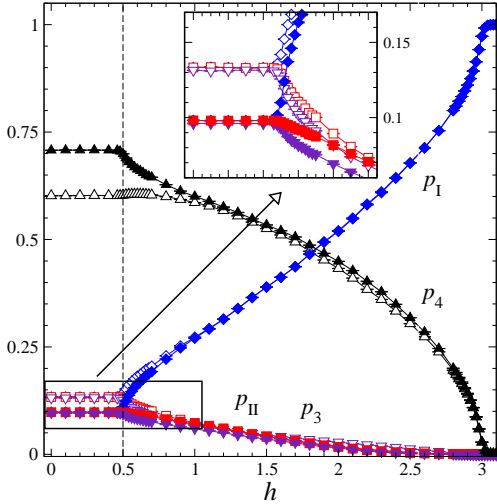


Fig. 7. Probabilities relative to the mixed basis versus the magnetic field h for the ladder Eq. (42): p_I (\diamond), p_{II} (\square), p_3 (\triangle), and p_4 (∇). Open (full) symbols are for n.n. spins along the same leg (on the same rung). The inset zooms in on the behavior of p_I , p_{II} , and p_3 near the critical field h_c .

rungs ($\gamma = 1$), the first excitations in the energy spectrum of the ladder are triplet excitations on the rungs.

When the Zeeman energy becomes larger than the gap, for $h > h_c$, the ground state starts to evolve with the field, whose immediate effect is that of pushing the quantities relative to spins on the rungs and along the legs towards each other: In fact, for $h > 1$ n.n. spins along the legs and on the rungs substantially share the same behavior. As for the probabilities, we see that p_{II} and p_3 keep being equivalent, no matter the value of the field, and slowly vanish as saturation is reached. On the contrary the probability for n.n. spins to be in $|u_1\rangle$ increases at the expense of the probability relative to the singlet state until, for $h \simeq 1.8$, the two probabilities cross each other.

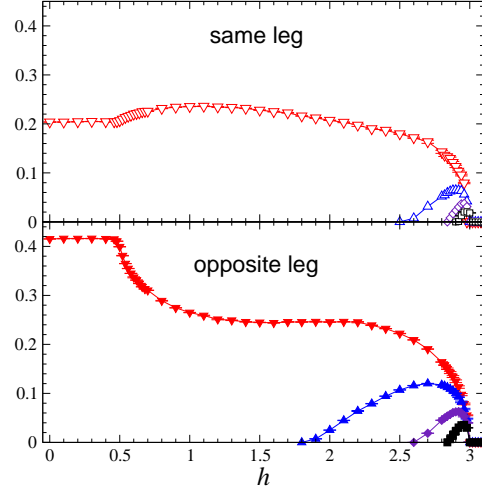


Fig. 8. From the upper to the lower curves: concurrences relative to spins belonging to the same (upper panel) and different legs (lower panel) versus field for the isotropic ladder up to $r = 4$.

Finally, we apply the formalism of Sec. 3 to extract features of the ground state from the concurrences. Fig. 8 shows the concurrences $C_{(r_i, r_\alpha)}$ up to the distance $r \equiv r_i + r_\alpha = 4$ for spins sitting on the same (upper panel) and on different legs (lower panel). The bipartite antiparallel entanglement between two spins sitting at a given distance r is in general larger on different legs, even beyond the n.n. case.

As expected, the field, after closing the gap, pushes $C_{(01)}$ and $C_{(10)}$ towards each other. Quite unexpectedly, however, this evolution includes a region where n.n. concurrence along the leg, $C_{(10)}$, increases. It is interesting to notice that $C_{(11)}$ switches on at $h \simeq 1.8$, where p_4 and p_I for n.n. spins are seen to cross each other in Fig. 6, signaling the crossover from an antiferromagnetic to a ferromagnetic-like configuration of the n.n. spins.

6 Conclusions

In this paper we developed a simple and effective formalism that allows to reconstruct the probability for two spins of a multi-spin system to be in a given quantum state, once the collective state of the system is given. Remarkably, such probabilities are found to be simple combination of standard magnetic observables, Eqs. (22-27). Within such formalism it is very natural to understand how concurrence quantifies the amount of entanglement between two spins by comparing the probabilities for those spins to be in different Bell states. In particular the expression for the concurrence clearly separates the case of parallel [Eq. (36)] and antiparallel [Eq. (39)] spins, leading to the introduction of the concept of *parallel* and *antiparallel* entanglement.

The knowledge of the probability distribution for a given set of two-spin states can be a useful tool to study quantum phases dominated by the formation of particular local two-spin states and to investigate the transitions

given by the alternation of such states. Within this class of phenomena we can cite the occurrence of short-range valence-bond states in low-dimensional quantum antiferromagnets [27], and the transition from a dimer-singlet phase to long-range order in systems of weakly coupled dimers under application of a field or by tuning of the inter-dimer coupling [28].

7 Acknowledgments

Fruitful discussions with L. Amico, G. Falci, S. Haas, D. Patanè, J. Siewert, and R. Vaia are gratefully acknowledged. We acknowledge support by SQUBIT2 project EU-IST-2001-390083 (A.F.), and by NSF under grant DMR-0089882 (T.R.).

References

1. M.C. Arnesen, S. Bose, and V. Vedral, Phys. Rev. Lett. **87**, 017901 (2001).
2. A. Osterloh, L. Amico, G. Falci, and R. Fazio, Nature (London) **416**, 608 (2002).
3. T.J. Osborne, and M.A. Nielsen, Phys. Rev. A **66**, 032110 (2002).
4. S. Ghosh, T.F. Rosenbaum, G. Aeppli, and S.N. Copper-smith, Nature (London) **425**, 48 (2003).
5. G. Vidal, J. I. Latorre, E. Rico, and A. Kitaev, Phys. Rev. Lett. **90**, 227902 (2003).
6. F. Verstraete, M. Popp, and J. I. Cirac, Phys. Rev. Lett. **92**, 027901 (2004).
7. T. Roscilde, P. Verrucchi, A. Fubini, S. Haas, and V. Tognetti, Phys. Rev. Lett. **93**, 167203 (2004); *ibid* **94**, 147208 (2005).
8. S. Hill and W.K. Wootters, Phys. Rev. Lett. **78**, 5022 (1997).
9. W.K. Wootters, Phys. Rev. Lett. **80**, 2245 (1998).
10. X. Wang and P. Zanardi, Phys. Lett. A **301**, 1 (2002).
11. O.F. Syljuåsen, Phys. Rev. A **68**, 060301 (2003).
12. U. Glaser, H. Büttner, and H. Fehske, Phys. Rev. A **68**, 032318 (2003).
13. L. Amico, A. Osterloh, F. Plastina, R. Fazio, and G. M. Palma, Phys. Rev. A **69**, 022304 (2004).
14. C. Bruder, R. Fazio, and G. Shön, Phys. Rev. B **47**, 342 (1993).
15. A. Anfossi, P. Giorda, A. Montorsi, and F. Traversa, Phys. Rev. Lett. **95**, 056402 (2005).
16. O. F. Syljuåsen and A.W. Sandvik, Phys. Rev. E **66**, 046701 (2002).
17. C. H. Bennett, D.P. DiVincenzo, J.A. Smolin, and W.K. Wootters, Phys. Rev. A **54**, 3824 (1996).
18. For instance, the factorized state $|u_1\rangle$ can be written as $|u_1\rangle = (|e_1\rangle + |e_2\rangle)/\sqrt{2}$, implying $p_1 = p_2 = 1/2$.
19. B.-Q. Jin and V.E. Korepin, Phys. Rev. A **69**, 062314 (2004).
20. T. Hikihara and A. Furusaki, Phys. Rev. B **69**, 064427 (2004).
21. W. Dür, G. Vidal, and J.I. Cirac, Phys. Rev. A **62**, 062314 (2000).
22. V. Coffman, J. Kundu, and W. K. Wootters, Phys. Rev. A **61** 053206 (2000).
23. T. J. Osborne and F. Verstraete, quant-ph/0502176.
24. T. Barnes, E. Dagotto, J. Riera, and E.S. Swanson, Phys. Rev. B **47**, 3196 (1993).
25. E. Dagotto, and T.M. Rice, Science **271**, 618 (1996).
26. G. Chaboussant, M.-H. Julien, Y. Fagot-Revurat, M. Hanson, L.P. Lévy, C. Berthier, M. Horvatić, and O. Piovesana, Eur. Phys. J. B **6**, 167 (1998).
27. S. R. White, R. M. Noack, and D. J. Scalapino, Phys. Rev. Lett. **73**, 886 (1994).
28. M. Matsumoto, B. Normand, T. M. Rice, and M. Sigrist, Phys. Rev. B **69**, 054423 (2004).